

Strip plasmons in a two-dimensional electron gas with grounded electrodes

A. Satou and V. Ryzhii

Computer Solid State Physics Laboratory, University of Aizu, Aizu-Wakamatsu 965-8580, Japan

Plasmons in two-dimensional electron gas (2DEG) strips with grounded electrodes (a gate or side contacts) are investigated. We consider two systems: (a) the 2DEG strip with a highly conducting gate and (b) the 2DEG strip with semi-infinite highly conducting side contacts. The systems are described by hydrodynamic equations coupled with the Poisson equation. Dispersion relations and ac electric potential distributions are obtained. We find the plasmon modes whose potential distributions, and hence electron density, are localized to the edges of the strip when the wave number of plasmons in the direction parallel to the strip is large. Frequencies of these strip modes are lower than those of infinite two-dimensional plasmons. The presence of grounded electrode(s) significantly modifies the plasmon dispersion relations.

I. INTRODUCTION

The spectrum of plasmons in electron systems depends on their dimensionality. In a bulk electron gas, the plasmon frequency, ω , is virtually independent of the wave vector, $\mathbf{q} = (q_x, q_y, q_z)$: $\omega \simeq \sqrt{4\pi e^2 n / m\epsilon_0}$, where e and m are the electron charge and effective mass, respectively, ϵ_0 is the dielectric constant, and n is the electron volume concentration. The spread in the electron velocities associated with the thermal movement of electrons or the degeneration of the electron system results in some dependence of ω on \mathbf{q} . However this dependence is rather weak [1]. Stern [2] and Chaplik [3] (see also early papers by Ritchie [4] and Ferrell [5]) discussed plasmons in the two-dimensional electron gas (2DEG) in the n -type inversion layer of metal-insulator-semiconductor structure. The dispersion relation for plasmons in 2DEG is given by [2] $\omega \propto \sqrt{q}$. Here $\mathbf{q} = (q_x, q_y)$ (z -axis is directed perpendicular to the 2DEG), and $q = |\mathbf{q}|$. Fetter [6] studied plasmons in the classical 2DEG on the surface of liquid He. The plasmons propagating along a one-dimensional wire (in the x -direction) correspond to [7, 8] $\omega \propto \sqrt{\ln(2/qa)}q$, where $q = q_x$ and a is the wire radius. The linear dispersion relation of 2DEG with a metallic gate has been found in Refs. 3 and 9. The first experimental observation of 2D plasmons in the 2DEG on liquid He was reported by Grimes and Adams [10]. Thereafter, Allen *et al.* [11] and Tsui *et al.* [12] observed far-infrared absorption and emission, respectively, in silicon inversion layers.

Edge plasmons in 2DEG with applied magnetic field, so-called edge magnetplasmons, were observed by Mast *et al.* [13, 14] and Glattli *et al.* [15]. Following their works, many theoretical investigations of edge magnetplasmons in bounded structures (semi-infinite half plane [16, 17, 18, 19, 20], disk [19, 21], and strip [19, 22]) were conducted using hydrodynamic electron transport models for 2DEGs coupled with self-consistent Poisson equation. The equations of these models produce integral equations which can be tackled by replacing their kernels with ones, or by expanding their solutions over complete sets of orthogonal functions (for comparison of these two methods see, for example, works by Fetter [17, 18]). Edge

plasmons in semi-infinite half plane with gate(s) were discussed by Fetter [17, 18] and Nazin *et al.* [23]. The discussion of early results on 2D plasmons can be found in the review papers by Theis [24] and Ando *et al.* [25].

Rudin and Dyakonov [26] considered the edge plasmons in the strip (strip plasmons) with zero magnetic field using a variational method, and found that two strip plasmon modes can exist in the strip structure (in Ref. 26 the lowest symmetric and antisymmetric modes were considered). However, to use their method, it is necessary to choose appropriate trial functions which are usually unknown and hard to find a priori, especially for complex structures with grounded electrodes.

In this paper, we calculate the spectra of plasmons propagating along strips of the 2DEG with closely located highly conducting grounded electrodes (a gate or side contacts), using the method developed in Refs. 27 and 28, in which the solution of the integral equation reduces to the eigenvalue problem. For simplicity and bearing in mind 2DEG in different systems like field-effect transistors, we consider 2DEG without magnetic field assuming the uniform electron equilibrium density and neglecting the gradient of pressure terms in the equation of motion [26]. We also neglect the electron collisions in 2DEG, which naturally leads to some modification of the plasmon dispersion relation [27] and results in some damping. The specifics of the geometry of the 2DEG systems in question and the charges induced by the perturbations of the electron density in the metallic region results in a modification of the plasmon spectra. We find the spatial distributions of the ac electric potential and the dependence of their spectra on the geometric parameters of the 2DEG system. In particular, we show that at sufficiently large wave numbers of the plasmons, their ac electric potential can be localized near both edges of the strip. For the 2DEG strip with metallic semi-infinite half-plane electrodes on its both sides, we find the higher strip plasmon modes.

Since the 2DEG systems similar to those studied in the paper can serve as resonant cavities and wave guides in different heterostructure devices operating in the terahertz range of frequencies [29], the results obtained below can be helpful of the development and optimization

of such devices.

II. EQUATIONS OF THE MODEL

We consider the following systems: (a) the 2DEG strip with a highly conducting gate of spacing W between them (gated cavity) and (b) the 2DEG strip with semi-infinite highly conducting side contacts (slot diode). The structure considered in Refs. 19, 22, and 26 can be considered as the structure (a) with $W \rightarrow \infty$. Schematic views of these structures are shown in Fig. 1.

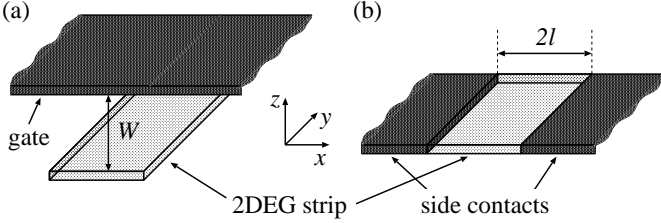


FIG. 1: Schematic views of structures under consideration: (a) gated cavity and (b) slot diode.

We use the hydrodynamic equations (the continuity equation and the Euler equation) to describe the electron transport:

$$\frac{\partial \Sigma}{\partial t} + \nabla \cdot (\Sigma \mathbf{u}) = 0, \quad (1)$$

$$\frac{\partial \mathbf{u}}{\partial t} + (\mathbf{u} \cdot \nabla) \mathbf{u} = \frac{e}{m} \nabla \varphi, \quad (2)$$

where $\Sigma = \Sigma(x, y, t)$ is the electron sheet concentration in the strip, $\mathbf{u} = \mathbf{u}(x, y, t)$ is the electron velocity, $\varphi = \varphi(x, y, z, t)$ is the electric potential, and e and m are electron charge and effective mass, respectively. \mathbf{u} is in xy -plane and $\nabla = (\partial/\partial x, \partial/\partial y)$. The hydrodynamic equations are coupled with the Poisson equation:

$$\frac{\partial^2 \varphi}{\partial x^2} + \frac{\partial^2 \varphi}{\partial y^2} + \frac{\partial^2 \varphi}{\partial z^2} = \frac{4\pi e}{\alpha} \Sigma \delta(z) \theta(l+x) \theta(l-x), \quad (3)$$

where α is the dielectric constant of the medium surrounding the strip, δ is the Dirac delta function, and θ is the Heaviside step function.

We consider the traveling wave with frequency ω and wave number q_y along y -axis, assuming that the potential (as well as other quantities) comprises both the dc and ac components: $\varphi(x, y, z, t) = \varphi_0(x, z) + \varphi_\omega(x, z) \exp[i(q_y y - \omega t)]$. Then, linearized version of Eqs. (1) and (2) together with Eq. (3) gives the following self-consistent equation:

$$\frac{\partial^2 \varphi_\omega}{\partial x^2} + \frac{\partial^2 \varphi_\omega}{\partial z^2} - q_y^2 \varphi_\omega = \frac{2l}{\pi \lambda_\omega} \left(\frac{\partial^2 \varphi_\omega}{\partial x^2} - q_y^2 \varphi_\omega \right) \delta(z) \theta(l+x) \theta(l-x), \quad (4)$$

where $\lambda_\omega = \omega^2/\Omega^2$ and $\Omega = \sqrt{2\pi^2 e^2 \Sigma_0 / m \alpha l}$ is the characteristic plasma frequency. Equation (4) can be reduced to the following:

$$\varphi_\omega(x, z) = -\frac{2l}{\pi \lambda_\omega} \int_{-l}^l dx' G(x, z; x', 0) \times \left(\frac{\partial^2}{\partial x'^2} - q_y^2 \right) \varphi_\omega(x', 0), \quad (5)$$

where $G(x, z; x', z')$ is the Green function which can be determined by the boundary conditions for each structure (boundary conditions and the Green function for each structure is introduced in subsequent sections).

For $|x| \leq l$ and $z = 0$, Eq. (6) is reduced to the following integral equation:

$$\varphi_\omega(x) = -\frac{2l}{\pi \lambda_\omega} \int_{-l}^l dx' G(x, 0; x', 0) \left(\frac{\partial^2}{\partial x'^2} - q_y^2 \right) \varphi_\omega(x'), \quad (6)$$

where $\varphi_\omega(x) = \varphi_\omega(x, 0)$. To solve Eq. (6), we expand $\varphi_\omega(x)$ in the cosine and sine series corresponding to symmetric and antisymmetric modes of potential, respectively. The series are different for each structure because boundary conditions at $|x| = l$ are different. Then, we can reduce the equation to the eigenvalue problem with an infinite matrix whose matrix elements are determined by the Green function G and the expansion. The problem can be solved numerically by truncating the matrix up to size N , evaluating its elements numerically, and then solving the eigenvalue problem with the finite matrix. Convergence of eigenvalues and eigenvectors was checked by increasing N , and we use the value $N = 100$ for all calculations done in the paper. An eigenvalue of the matrix, λ_ω , gives the plasma frequency of a mode

$$\omega = \sqrt{\lambda_\omega} \Omega. \quad (7)$$

III. STRIP PLASMONS IN A GATED CAVITY

Since electrons in the 2DEG strip of a gated cavity cannot go outside, the x -component of their velocity at edges of the strip must be zero, i.e., in terms of the potential, $\partial \varphi_\omega / \partial x|_{z=0, |x|=l} = 0$. Consequently, the Green function for a gated cavity is

$$\begin{aligned} & G^{(GC)}(x, z; x', z') \\ &= \frac{1}{2\pi} K_0 \left(q_y \sqrt{(x - x')^2 + (z - z')^2} \right) \\ & \quad - \frac{1}{2\pi} K_0 \left(q_y \sqrt{(x - x')^2 + (z - z' - 2W)^2} \right), \end{aligned} \quad (8)$$

where the first term of Eq. (8) is the Green function for a free cavity. The expansions which satisfy the boundary conditions are the following:

$$\varphi_\omega^{(s)}(x) = \frac{c_0}{\sqrt{2}} + \sum_{k=1}^{\infty} c_k^{(s)} \cos(q_{2k} x) \quad (9)$$

for symmetric modes and

$$\varphi_{\omega}^{(a)}(x) = \sum_{k=1}^{\infty} c_k^{(a)} \sin(q_{2k-1}x) \quad (10)$$

for antisymmetric modes, where $q_n = n\pi/2l$. The effective wave number corresponding to the x -direction is equal to q_{2n} for n -th symmetric mode (as a special case, zero-th mode correspond to $q_{2n} = 0$) and to q_{2n-1} for n -th antisymmetric mode. Substituting Eqs. (9) and (10) into Eq. (6) and using the orthonormality of each term in expansions, we arrive at the following eigenvalue problem:

$$\sum_{k'=0}^{\infty} \theta_{kk'}^{(s)} c_{k'}^{(s)} = \lambda_{\omega}^{(s)} c_k^{(s)} \quad (11)$$

for symmetric modes, where $k = 0, 1, 2, \dots$ and

$$\theta_{00}^{(s)} = \frac{1}{\pi} (q_y l)^2 \int_{-1}^1 d\xi \int_{-1}^1 d\xi' G^{(GC)}(\xi, \xi'), \quad (12)$$

$$\theta_{k0}^{(s)} = \frac{\sqrt{2}}{\pi} (q_y l)^2 \int_{-1}^1 d\xi \int_{-1}^1 d\xi' G^{(GC)}(\xi, \xi') \times \cos(q_{2k} l \xi) \quad (13)$$

when $k > 0$,

$$\theta_{0k'}^{(s)} = \frac{\sqrt{2}}{\pi} [(q_{2k'} l)^2 + (q_y l)^2] \int_{-1}^1 d\xi \int_{-1}^1 d\xi' G^{(GC)}(\xi, \xi') \times \cos(q_{2k'} l \xi') \quad (14)$$

when $k' > 0$, and

$$\theta_{kk'}^{(s)} = \frac{2}{\pi} [(q_{2k'} l)^2 + (q_y l)^2] \int_{-1}^1 d\xi \int_{-1}^1 d\xi' G^{(GC)}(\xi, \xi') \times \cos(q_{2k} l \xi) \cos(q_{2k'} l \xi') \quad (15)$$

when $k, k' > 0$. For antisymmetric modes, we obtain

$$\sum_{k'=1}^{\infty} \theta_{kk'}^{(a)} c_{k'}^{(a)} = \lambda_{\omega}^{(a)} c_k^{(a)}, \quad (16)$$

where $k = 1, 2, 3, \dots$ and

$$\theta_{kk'}^{(a)} = \frac{2}{\pi} [(q_{2k'-1} l)^2 + (q_y l)^2] \int_{-1}^1 d\xi \int_{-1}^1 d\xi' G^{(GC)}(\xi, \xi') \times \sin(q_{2k-1} l \xi) \sin(q_{2k'-1} l \xi'). \quad (17)$$

Here we use the notation $G^{(GC)}(\xi, \xi') = G^{(GC)}(l\xi, 0; l\xi', 0)$. The details of numerical computation of Eqs. (12)-(15) and (17) are discussed in the Appendix.

Figure 2 shows the dispersion relation calculated for a free cavity. The dotted line is the dispersion relation of infinite 2D plasmons which is given by $\omega_p = \sqrt{q_y l / \pi} \Omega$.

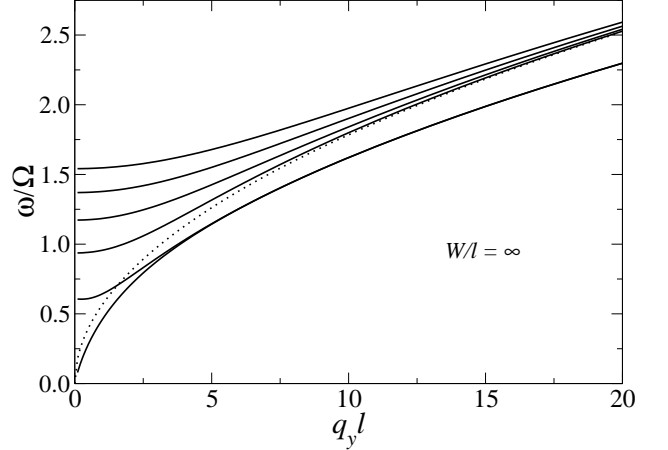


FIG. 2: Dispersion relation for a free cavity ($W/l \rightarrow \infty$) with $q_nl/\pi = 0, 1/2, 1, 3/2, 2, 5/2$. Solid lines with lowest frequencies through highest ones correspond to $q_nl/\pi = 0$ through $q_nl/\pi = 5/2$. The dotted line is the dispersion relation of infinite 2D plasmons. Two modes whose frequencies are lower than those of infinite 2D plasmons for $q_y l \gg 1$ are identified as strip plasmon modes.

Frequencies in the limit $q_y l \rightarrow 0$ coincide with those calculated for standing plasma waves in a free cavity in Ref. 28. It can be seen from Fig. 2 that the lowest symmetric and antisymmetric modes have lower frequencies than those of infinite 2D plasmons for $q_y l \gg 1$, while frequencies of higher modes approach to those of infinite 2D plasmons. These two modes are identified as strip plasmons, as is also evident from their potential distributions (Fig. 3). This phenomenon was already discussed theoretically in the case of a semi-infinite half-plane [18] and in the case of a free cavity [26]. For $q_y l \gg 1$, the effect of one edge on another can be neglected, and the difference between symmetric and antisymmetric modes becomes unimportant. The lowest modes in our case are equivalent to an edge mode in the case of a half-plane. The dispersion curves for lowest symmetric and antisymmetric modes are identical with those obtained in Ref. 26. The higher modes seem to correspond to the normal wave-like modes in x -direction whose frequencies are proportional to $\sqrt{q_n^2 + q_y^2}$ because the effective wave number q_n can be considered to take continuous value when $q_y l \gg 1$.

The dispersion relation for plasmons in a gated cavity is illustrated in Fig. 4. For the zero-th symmetric mode ($q_nl/\pi = 0$), one can see that, as W/l decreases, the plasma frequencies decrease and their dependence on $q_y l$ becomes linear. When $q_y \gg 1/W$, the effect of the gate is small and the frequencies approach to those for a free cavity (see curves for $W/l = 0.1$). For the first symmetric mode ($q_nl/\pi = 1$) the dependence is more complicated due to nonzero frequency of plasmons in the limit $q_y l \rightarrow 0$ and its dependence of W/l [28]. Figure 5 shows the plasma frequencies as a function of W/l for fixed $q_y l$. For $q_y l = 1$, the influence of the gate on the fre-

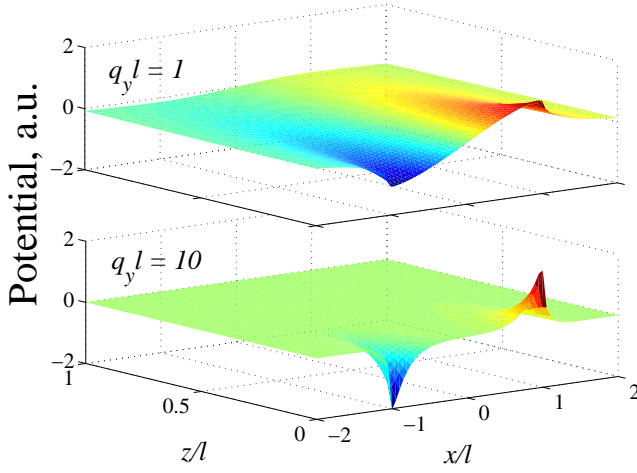


FIG. 3: Potential distributions of lowest antisymmetric mode for a free cavity with $q_y l = 1$ (above) and $q_y l = 10$ (below). The localization of potential at the edges of the 2DEG strip becomes apparent for $q_y l \gg 1$.

quencies is gradual, i.e., the frequencies slowly decrease with decreasing W/l and tend to zero as $W/l \rightarrow 0$. On the contrary, for $q_y l = 10$, the change in the frequency from zero to the value corresponding to $W/l \rightarrow \infty$ is more rapid. It is also worth mentioning that for $q_y l = 1$ the frequency differences between lowest and second lowest symmetric and antisymmetric modes are significant whereas they are not the case for $q_y l = 10$.

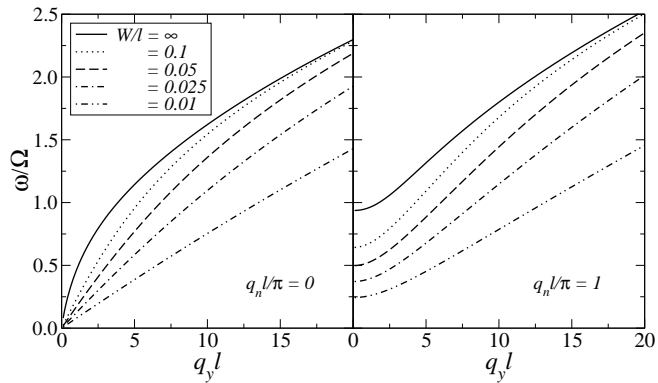


FIG. 4: Dispersion relation for a gated cavity with $q_n l / \pi = 0, 1$ and $W/l = 0.01, 0.025, 0.05, 0.1, \infty$.

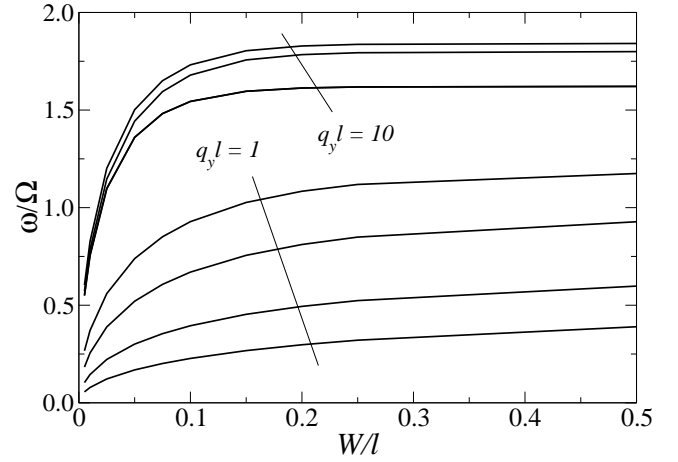


FIG. 5: Plasma frequency vs the ratio W/l with $q_y l = 1, 10$ and different $q_n l / \pi$ for a gated cavity. For each $q_y l$, four solid lines with lowest frequency through highest ones correspond to $q_n l / \pi = 0, 1/2, 1, 3/2$. For $q_y l = 10$, curves for $q_n l / \pi = 0$ and $q_n l / \pi = 1/2$ are indistinguishable.

IV. EDGE PLASMONS IN A SLOT DIODE

For a slot diode, the boundary conditions are given by $\varphi_\omega|_{|x| \geq l, z=0} = 0$, and the relevant Green function is

$$\begin{aligned} & G^{(SD)}(x, z; x', z') \\ &= \frac{1}{2\pi} \sum_{n=-\infty}^{\infty} K_0 \left(q_y l \sqrt{(\theta - \theta' - 2n\pi)^2 + (\psi - \psi')^2} \right) \\ & \quad - \frac{1}{2\pi} \sum_{n=-\infty}^{\infty} K_0 \left(q_y l \sqrt{(\theta + \theta' - 2n\pi)^2 + (\psi - \psi')^2} \right), \end{aligned} \quad (18)$$

where $\theta + i\psi = \cos^{-1}[(x + iz)/l]$ and $\theta' + i\psi' = \cos^{-1}[(x' + iz')/l]$. When evaluating Eq. (18) numerically, series are cut at appropriately large n , so that the n -th term can be neglected. Using the expansion

$$\varphi_\omega^{(s)}(x) = \sum_{k=1}^{\infty} c_k^{(s)} \cos(q_{x,2k-1} x) \quad (19)$$

for symmetric modes and

$$\varphi_\omega^{(a)}(x) = \sum_{k=1}^{\infty} c_k^{(a)} \sin(q_{x,2k} x) \quad (20)$$

for antisymmetric modes, we arrive at the eigenvalue problem similar to Eqs. (11) and (16) [only a difference is that the indices k and k' start from 1 in Eq. (11)] with the matrix elements

$$\begin{aligned} \theta_{kk'}^{(s)} &= \frac{2}{\pi} [(q_{2k'-1} l)^2 + (q_y l)^2] \int_{-1}^1 d\xi \int_{-1}^1 d\xi' G^{(SD)}(\xi, \xi') \\ & \quad \times \cos(q_{2k-1} l \xi) \cos(q_{2k'-1} l \xi') \end{aligned} \quad (21)$$

for symmetric modes and

$$\theta_{kk'}^{(a)} = \frac{2}{\pi} [(q_{x,2k'}l)^2 + (q_y l)^2] \int_{-1}^1 d\xi \int_{-1}^1 d\xi' G^{(SD)}(\xi, \xi') \times \sin(q_{x,2k'}l\xi) \sin(q_{x,2k'}l\xi'). \quad (22)$$

Solving the eigenvalue problems numerically and substituting eigenvalues into Eq. (7), dispersion relation for a slot diode is obtained (Fig. 6). Frequencies in the limit $q_y l \rightarrow 0$ coincide with those calculated for standing plasma waves in a slot diode in Ref. 28. Aside from the first modes, we have found that higher strip modes can exist. By observing the potential distributions, it was turned out that the potential distribution of a mode begins to change and be localized near the edges of the 2DEG strip at the wave number q_y at which the dispersion relation curve of the mode crosses over the curve of infinite 2D plasmons. One can also see from Fig. 6 that dispersion relation curves of symmetric and anti-symmetric modes with same index begin to coincide at this wave number. Figure 7 shows potential distributions of symmetric modes for $q_n l / \pi = 1/2, 3/2$, and $5/2$ with $q_y l = 30$. From Fig. 7, one can see the increasing of peak numbers as $q_n l / \pi$ increases, and peaks become larger and wider as they are farther from an edge of the 2DEG strip.

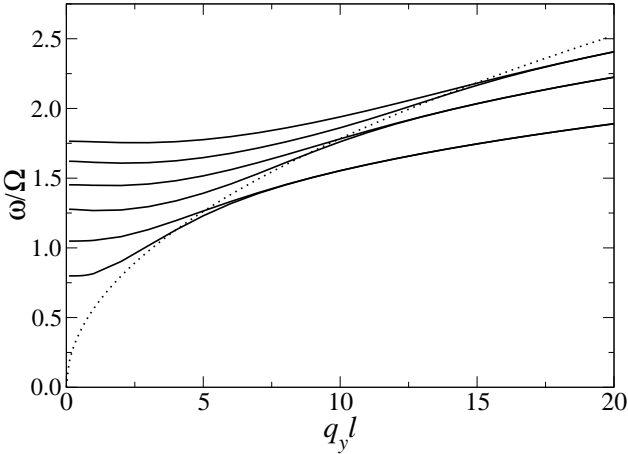


FIG. 6: Dispersion relation for a slot diode with $q_n l / \pi = 1/2, 1, 3/2, 2, 5/2, 3$. Solid lines with lowest frequencies through highest ones correspond to $q_n l / \pi = 1/2$ through $q_n l / \pi = 3$. The dotted line is the dispersion relation of infinite 2D plasmons.

V. CONCLUSIONS

In summary, we have studied plasmons in the following 2D systems: (a) the 2DEG strip with a highly conducting gate (gated cavity) and (b) the 2DEG strip with semi-infinite highly conducting side contacts (slot diode). We have found the dispersion relations of the plasmons and

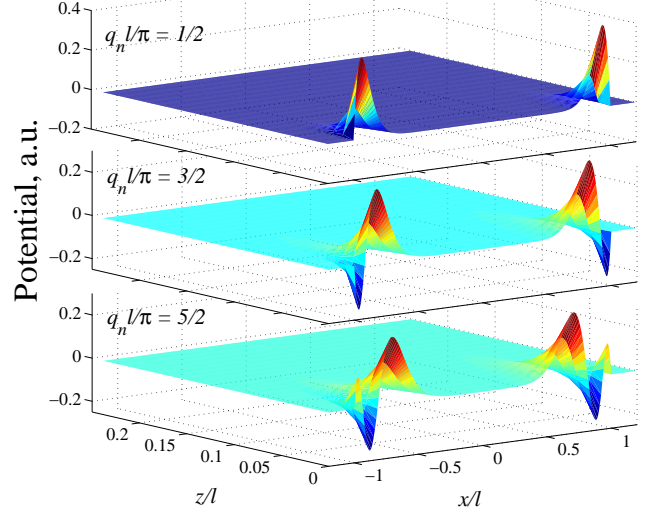


FIG. 7: Potential distributions of three symmetric modes ($q_n l / \pi = 1/2, 3/2$, and $5/2$) with $q_y l = 30$. These strip modes have two, four, and six peaks, respectively.

the spatial distributions of ac electric potential. In particular, it has been shown that at sufficiently large wave numbers of plasmons, their ac electric potential of some modes can be localized near both edges of the strip, and their frequencies are lower than those of infinite 2D plasmons.

Acknowledgements

The authors are thankful to A. Chaplik and M. S. Shur for numerous discussions.

APPENDIX

Eqs. (12) through (14) can be reduced to the following simpler expressions which contain only single integrals:

$$\theta_{00}^{(s)} = \frac{2}{\pi} (q_y l)^2 \{ K_0(2q_y l) \mathcal{L}_{-1}(2q_y l) + K_1(2q_y l) \mathcal{L}_0(2q_y l) - [1 - 2q_y l K_1(2q_y l)] / 2\pi (q_y l)^2 - \frac{1}{\pi} \int_0^2 d\xi \left(1 - \frac{\xi}{2} \right) K_0 \left(q_y l \sqrt{\xi^2 + a^2} \right) \}, \quad (A.1)$$

where K_n is the modified Bessel function of second kind, \mathcal{L}_n is the modified Struve function [30], and $a = 2W/l$,

$$\theta_{k0}^{(s)} = (-1)^{k+1} \frac{2\sqrt{2}}{\pi^2 k} (q_y l)^2 \int_0^2 G^{(GC)}(\xi) \sin(k\pi\xi), \quad (A.2)$$

and

$$\theta_{0k'}^{(s)} = (-1)^{k'+1} \frac{2\sqrt{2}}{\pi^2 k'} [(k'\pi)^2 + (q_y l)^2] \times \int_0^2 G^{(GC)}(\xi) \sin(k'\pi\xi). \quad (A.3)$$

Here, $G^{(GC)}(\xi) = G^{(GC)}(\xi, 0)$. Eq. (15) can be reduced to

$$\theta_{kk}^{(s)} = -\frac{2[(k\pi)^2 + (q_y l)^2]}{k\pi^2} \int_0^2 d\xi S_k(\xi) \quad (\text{A.4})$$

and

$$\theta_{kk'}^{(s)} = (-1)^{k+k'+1} \frac{4[(k'\pi)^2 + (q_y l)^2]}{(k^2 - k'^2)\pi^3} [T_k(2) - T_{k'}(2)] \quad (\text{A.5})$$

when $k \neq k'$. Similarly, Eq. (17) can be reduced to

$$\theta_{kk}^{(a)} = -\frac{2[(h\pi)^2 + (q_y l)^2]}{h\pi^2} \int_0^2 d\xi S_h(\xi) \quad (\text{A.6})$$

and

$$\theta_{kk'}^{(a)} = (-1)^{k+k'+1} \frac{4[(h'\pi)^2 + (q_y l)^2]}{(h^2 - h'^2)\pi^3} [T_h(2) - T_{h'}(2)], \quad (\text{A.7})$$

where $h = (2k - 1)/2$ and $h' = (2k' - 1)/2$, when $k \neq k'$. Here,

$$S_\nu(\xi) = \int_0^\xi d\xi' \sin(\nu\pi\xi') \frac{d}{d\xi'} G^{(GC)}(\xi') \quad (\text{A.8})$$

and

$$T_\nu(\xi) = \int_0^\xi d\xi' [\cos(\nu\pi\xi') - 1] \frac{d}{d\xi'} G^{(GC)}(\xi'). \quad (\text{A.9})$$

Since all integrands of integrations in Eqs. (A.1) through (A.9) have no singularity, the Gaussian quadrature [31] was used to perform the numerical integrations.

On the other hand, since Eq. (18) is very complicated, we directly performed double integrations in Eqs. (21) and (22) after integrating them by parts:

$$\begin{aligned} \theta_{kk'}^{(s)} = & \frac{2q_{2k-1}l}{\pi} [(q_{2k'-1}l)^2 + (q_y l)^2] \\ & \times \int_{-1}^1 d\xi \int_{-1}^1 d\xi' \mathcal{G}^{(SD)}(\xi, \xi') \sin(q_{2k-1}l\xi) \cos(q_{2k'-1}l\xi') \end{aligned} \quad (\text{A.10})$$

and

$$\begin{aligned} \theta_{kk'}^{(a)} = & -\frac{2q_{2k}l}{\pi} [(q_{2k'}l)^2 + (q_y l)^2] \\ & \times \int_{-1}^1 d\xi \int_{-1}^1 d\xi' \mathcal{G}^{(SD)}(\xi, \xi') \cos(q_{2k}l\xi) \sin(q_{2k'}l\xi'), \end{aligned} \quad (\text{A.11})$$

where $\mathcal{G}^{(SD)}(\xi, \xi') = \int_{-1}^\xi G^{(SD)}(t, \xi') dt$. Since $G^{(SD)}$ has logarithmic singularity at $\xi = \xi'$, $\mathcal{G}^{(SD)}$ is the continuous function of ξ and ξ' . $\mathcal{G}^{(SD)}$ was calculated using adaptive quadrature [31]. Finally, Eqs. (A.10) and (A.11) were calculated by Simpson's double integral method [31].

[1] E. M. Lifshitz and L. P. Pitaevskii, *Physical Kinetics* (Pergamon, Oxford, 1981), Sects. 31 and 32.
[2] F. Stern, Phys. Rev. Lett. **18**, 546 (1967).
[3] A. V. Chaplik, Zh. Eksp. Teor. Fiz. **63**, 746 (1972) [Sov. Phys.-JETP **35**, 395 (1972)].
[4] R. H. Ritchie, Phys. Rev. **106**, 874 (1957).
[5] R. A. Ferrell, Phys. Rev. **111**, 1214 (1958).
[6] A. L. Fetter, Phys. Rev. B **10**, 3739 (1974).
[7] R. A. Ferrell, Phys. Rev. Lett. **13**, 330 (1964).
[8] A. Gold and A. Ghazali, Phys. Rev. B **41**, 7626 (1990).
[9] A. Eguiluz, T. K. Lee, J. J. Quinn, and K. W. Chiu, Phys. Rev. B **11**, 4989 (1975).
[10] C. C. Grimes and G. Adams, Phys. Rev. Lett. **36**, 145 (1976).
[11] S. J. Allen, D. C. Tsui, and R. A. Logan, Phys. Rev. Lett. **38**, 980 (1977).
[12] D. C. Tsui, E. Gornik, and R. A. Logan, Solid State Commun. **35**, 875 (1980).
[13] D. B. Mast and A. J. Dahm, Physica **126B**, 457 (1984).
[14] D. B. Mast, A. J. Dahm, and A. L. Fetter, Phys. Rev. Lett. **54**, 1706 (1985).
[15] D. C. Glattli, E. Y. Andrei, G. Deville, J. Poitrenaud, and F. I. B. Williams, Phys. Rev. Lett. **54**, 1710 (1985).
[16] J.-W. Wu, P. Hawrylak, and J. J. Quinn, Phys. Rev. Lett. **55**, 879 (1985).
[17] A. L. Fetter, Phys. Rev. B **32**, 7676 (1985).
[18] A. L. Fetter, Phys. Rev. B **33**, 3717 (1986).
[19] V. A. Volkov and S. A. Mikhailov, Zh. Eksp. Teor. Fiz. **94**, 217 (1988) [Sov. Phys. JETP **67**, 1639 (1988)].
[20] X. Xia and J. J. Quinn, Phys. Rev. B **50**, 11187 (1994).
[21] A. L. Fetter, Phys. Rev. B **33**, 5221 (1986).
[22] V. Cataudella and G. Iadonisi, Phys. Rev. B **35**, 7443 (1987).
[23] S. S. Nazin, N. I. Shikina, and V. B. Shikin, Zh. Eksp. Teor. Fiz. **92**, 1648 (1987) [Sov. Phys. JETP **65**, 924 (1987)].
[24] T. N. Theis, Surf. Sci. **98**, 515 (1980).
[25] T. Ando, A. B. Fowler, and F. Stern, Rev. Mod. Phys. **54**, 437 (1982).
[26] S. Rudin and M. Dyakonov, Phys. Rev. B **55**, 4684 (1997).
[27] V. Ryzhii, A. Satou, I. Khmyrova, A. Chaplik, and M. S. Shur, J. Appl. Phys. **96**, 7625 (2004).
[28] A. Satou, I. Khmyrova, A. Chaplik, V. Ryzhii, and M. S. Shur, Jpn. J. Appl. Phys. **44**, 2592 (2005).
[29] M. S. Shur and V. Ryzhii, Int. J. High Speed Electron. Syst. **13**, 575 (2003).
[30] M. Abramowitz and I. A. Stegun, *Handbook of mathematical functions*, (Dover, New York, 1965), Chaps. 9 and 12.
[31] R. L. Burden and J. D. Faires, *Numerical Analysis* (PWS Publishing, Boston, 1993), Chap. 4.